Arch. Metall. Mater. **70** (2025), 1, 317-324

DOI: https://doi.org/10.24425/amm.2025.152548

B.K. KIPSANG[1], K. WACŁAWIAK[1*], WIM DE WAELE[2]

IMPLEMENTATION OF RECENT ADVANCES IN FRACTURE TOUGHNESS TESTING TO INVESTIGATE TEARING RESISTANCE OF HEAT-RESISTANT STEEL 14MoV6-3

Since WWII, progress has been made in understanding how materials fail and how to prevent such failures. In this work, the newly standardized Single Edge Notch Tension (SENT) specimen is used to assess the ductile tearing resistance of 14MoV-3 steel. Crack Tip Opening Displacement (CTOD90) is measured using Unloading Compliance (UC) and Direct Current Potential Drop methods (DCPD) to measure crack growth. The tearing resistance curves were determined for the new as-received samples and after degradation by creeping. The maximum loads, the CTOD at crack initiation, and resistance curves were compared for each ageing stage. As-received specimens resulted in the highest CTOD90 compared to the creep-degraded specimens. DCPD provided a better crack prediction compared to UC.

Keywords: CTOD; tearing elastic compliance; single-edge notched tension (SENT) specimen; 14MoV6-3 steel; DCPD method

1. Introduction

Cracks in boiler elements form during long-term operation under cyclic loads and environmental factors [1]. For 14MoV6-3 steel there is the likelihood of these cracks to shift in fracture mechanism from ductile to cleavage [2]. Boiler tube creep fractures are thought to be the cause of 10% of all power plant failures. In thermal power equipment and other major steam pipes, metallographic analysis and hardness measurements are routinely employed to determine the technical status of operated steels. Steel structure research focuses largely on grain and carbide size, carbide distribution inside grains and along their borders, and pore density.

An accurate determination of fracture toughness is critical for assessing equipment failure. Early fracture assessments relied on the energy approach, which defined fracture as occurring when the energy available for crack growth is sufficient to overcome the material's resistance [3].

Previous research initiatives on the fracture behaviour of 14MoV6-3 were done using SENB and CT specimens which provide over-conservative figures due to their high crack tip constraint. However, the fracture behaviour of 14MoV6-3 employing SENT specimens after a lengthy period of operations is still absent. Studies found that the SENT specimen provide a reasonable match to the constraint conditions of a circumferential crack in a pipe under strain-based design conditions [4]. Specimen geometry and mode of forces influence the degree of crack tip constraint [5]. Lowering the constraint increases fracture toughness, and vice versa [6]. Graba [7] reported that in-plane geometric constraints represented by Q-stresses on the crack tip opening displacement for SENB specimens subjected to primarily plane strain conditions affect toughness values. The effect of specimen geometry on the CTOD value is presented by Kowalski [8]. The presented findings indicate that specimen cross-section geometry significantly affects CTOD. Kang et. al [9] established that different specimen geometries have different crack tip constrains.

Modern steels are becoming increasingly tough hence K_I cannot be used to characterize fracture, instead EPFM is applied represented by CTOD or J-integral as a function of the ductile crack extension Δa, in mm [4]. Of the two parameters CTOD have been used the most [5]. Promising results on the feasibility of spirally welded pipes to be used in a strain-based design context have been reported in [10].

Creep strength and fracture resistance are the most important determinants of the appropriateness of high-pressure steam pipeline materials [11]. Creep is to blame for 30% of all tube failures in boilers [12]. According to a survey [13] it was reported

[1] SILESIAN UNIVERSITY OF TECHNOLOGY, DEPARTMENT OF MATERIALS TECHNOLOGIES, 2A AKADEMICKA STR., 44-100 GLIWICE, POLAND
[2] DEPARTMENT OF ELECTROMECHANICAL, SYSTEMS AND METAL ENGINEERING, GHENT UNIVERSITY, BELGIUM

* Corresponding author: krzysztof.waclawiak@polsl.pl

that literature data do not provide much information on low-alloy energy steels concerning service life. Considering the wide use of 14MoV6-3 steel for many components of power boilers at temperatures up to 540°C efforts have been put to research the effect of creep and long term operation on 14MoV6-3 steel [1,2], but no literature could be found to measure resistance curves after long periods of operations. In a study by [13] degradation of microstructure and strength properties of heat-resistant steels operating under variable loads was investigated. Considering this, it is critical to get more insights on the influence of creep ageing on the fracture toughness of materials used in power industry infrastructure and materials extracted from power plants. Research by [14] experimented on impacts of exploitation time and temperature on resistance to brittle fracture of low-alloyed Cr-Mo steel A-387 Gr. They concluded that exploitation time impacted the resistance to crack propagation and other mechanical properties.

Early service termination is the result of a complex stress state that includes torsion and/or bending components. To forecast the date of the next technical inspection, decommissioning or to fully justify equipment to continue operating in the presence of a crack or after the end of its design lifetime, conventional evaluation of durability uses metallographic tests of structure degradation as well as to check with the magnetic or ultrasonic method to asses structural integrity [15]. The material's fracture behavior data are required for integrity assessment due to their loading range [16]. This ensures the prevention of brittle fracture In this work the main objective is the assessment of tearing resistance in steel that has been subjected to turbine operating conditions. Depending on their loading range results may be used for estimation of operational reliability forecast in the presence of a crack. The results also can be correlated to indentation-based fracture toughness testing and correlation factor used to predict future fracture strength during continuous operation.

2. Materials and methods

2.1. Materials

The study was carried out using 14MoV6-3 steel. The materials were delivered from Třinecké železárny (Třinec, Czech Republic). The samples were extracted from the round bars in the longitudinal direction ensuring material anisotropy. The chemical composition according to manufacture's product certificates is presented in TABLE 1.

TABLE 1

Chemical composition of the 14MoV6-3 steel according to manufacturer's certificates [weight %]

Element	C	Mn	Si	P	S	Cr	Al	Mo	V
%	0.15	0.61	0.24	0.03	0.007	0.60	0.018	0.453	0.318

2.2. Fracture toughness testing employing SENT specimens

The SENT specimen geometry has been found to have almost similar but slightly higher constrain with thin walled structures under tension [6,17]. In the year 2014 the BS 8571 standard [18] was published as a test method employing SENT specimen. The CTOD can be measured directly from the mouth of the specimen or estimated from a clip gauge extensometer. It uses standardized specimens as shown in Fig. 1, the specimen can be loaded by either clamping or pins.

Fracture toughness testing was performed using SENT specimens all having dimensions of $B = W = 10$ mm and the daylight grip length (H) is equivalent to 10 W and $a/W = 0.5$. The use of deeply cracked specimens of a/$W = 0.5$ is to guarantee conditions leading to high crack-tip constraint with limited scale plasticity [19] and to compare the results with previous work in the literature. A two-step milling procedure was used to machine the initial cracks such that the final root radius of the crack was 0.15 mm. Four holes of diameter 1.9 mm and 3 mm depth were drilled 4.5 mm from the notch for attaching the clip gauges as shown in Fig. 1.

Wang et al. [20] compared methods for computing J and CTOD and proposed a complementary plastic η factor (η_{pl}) which is affected by dimension ratios. The absolute error in this new method was reduced to less than 10%. This approach is a useful and accurate method for predicting η_{pl} values for clamped SENT specimens with $0.3 \leq a/W \leq 0.7$ and $B/W = 1$ and 2.

2.3. Creeping and codeing of the specimens

The specimens where creeped at 540°C with the intention of simulating the degradation caused by working conditions in the power plants. The degradation was done using Kappa 05DS Zwick machine fitted with a furnace. The creep pressure was 169 MPa for the three stages of ageing namely 120, 240, and 480 hours. This represented 10% of the expected lifespan. The new uncreeped specimens where code named NS1, NS2 and

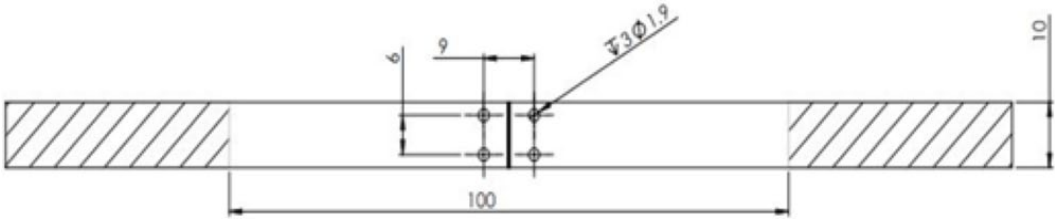

Fig. 1. Schematic drawing (out-of-scale) showing the dimensions of the SENT test specimen

NS3. The 120 hours ageing creep where code named 10-120 and 12-120, the240 hours creep ageing where code named 3-240, 6-240 and 6-240 dot while the 480 hours creep ageing were code named 4-480, 5-480 and 7-480.

2.4. SENT tearing resistance test procedure

No fatigue pre-cracking was done since this would make controlling the initial fracture depth more difficult, and it is not necessary for ductile materials [17]. The test setup is as shown in Fig. 2. The current pins on the specimen were positioned to ensure a uniform potential field hence the potential drop across the crack is independent of the pin's location.

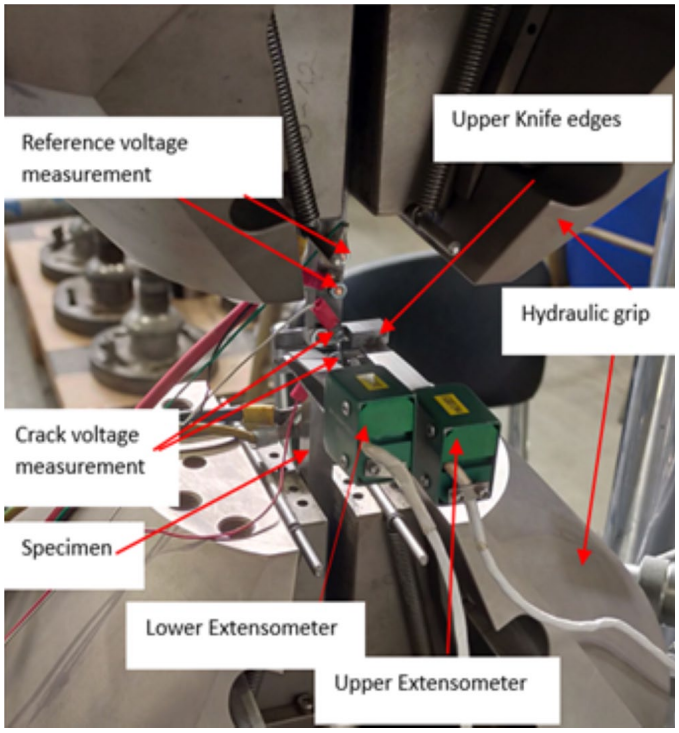

Fig. 2. The SENT specimen testing setup

The tests were carried out at room temperature at Soete Laboratory at Ghent University using a 100 kN servo hydraulic testing machine. The clamping approach for griping was used using pressure of 5 MPa to prevent introducing unnecessary stresses during gripping. Tensile loading was applied to the specimen under quasi-static displacement control at a loading rate of 0.01 mm/s [17]. A double clip gauge approach was used to compute the crack mouth opening displacement (CMOD) according to the procedure described in literature [21]. The crack growth was measured using both the direct current potential drop method (DCPD) and unloading compliance (UC). The supplied current was 25 A ensuring there is high current density given the good conductivity of steel. The unloading regime was done following the procedures by ASTM E1820-18a [22].

After attaining a load level equal to half of F_m, where F_m is given by Eq. (1). Six unloading cycles in the elastic regime were performed in each test to allow the specimen to "bed in" as described in ISO standards [23].

$$F_m = \frac{1}{2}\frac{\sigma_{0.2} + \sigma_{UTS}}{2}\left(W - a_o\right)B_e \tag{1}$$

where: F_m is the maximum foece before unloading, B is the specimen thickness, B_e is the effective specimen thickness incase there is side grooves, W is specimen width, a_o is the original crack length, $\sigma_{0.2}$ i the yield strenght and σ_{UTS} is the ultimate strenght In this case $B_e = B$ since there were no side grooves. The unloading at the plastic region was done after equal crack openings. The tests were carried out past the maximum load until the load fell below 80% of the maximum measured value to acquire enough fracture development. There are three definitions for CTOD [24]. For this work, the 90° intercept method also called the UGent method [24] is applied. The *CTOD* was calculated from the double clip gauge data performed using Eq. (2) as described in [22].

$$CTOD = 2\frac{V_2\left(a_O + h_1\right) - V_1\left(a_O + h_2\right)}{\left(V_2 - V_1\right) - 2\left(h_2 - h_1\right)} \tag{2}$$

For the estimation of crack growth using the unloading compliance, the correction factor (F) as suggested by [23] is applied. Compliance to crack size is expressed as a ratio of a/W as presented in Eq. (3).

$$\frac{a_i}{W} = 1.6485 - 9.1005U_i + 33.025U_i^2 - 78.467U_i^3 + 97.344U_i^4 - 47.227U_i^5 \tag{3}$$

where: U is expressed in Eq. (4) as.

$$U = \frac{1}{1 + \sqrt{B_{ef} C_{icorr,i} E}} \tag{4}$$

where: E is the Young's modulus, $C_{icorr,i}$ is the corrected compliance and B_{ef} is the effective thickness which in our case equals B because there are no side grooves.

The fracture surfaces of the studied specimens were heat tinted in an oven at 200°C for 2 hours to analyze them. They were then cooled in liquid nitrogen before being brittle fractured. The nine-point average technique was used to get an average final crack length. This was used to validate the crack length measurement obtained by UC and DCPD.

Tensile tests were performed to characterize the mechanical properties of the as received and the creep aged materials. Hereto, round bar specimens with a gauge diameter and gauge length of 6 mm and 4 mm respectively were used. At least two specimens were tested for each ageing condition using Zwick/Roel Z100 universal testing machine. Testing was done according to ASTM standard [25]. A clip-on extensometer was used to record load elongation data in the elastic zone.

3. Results and discussion

3.1. Mechanical properties

Fig. 3 presents the stress-strain curves for the new and aged specimens tested at room temperature. The characteristics of obtained tensile curves at room temperature correspond to typical stress strain curve of ductile metallic material even after the longest period of ageing which is 480 hours. Tensile testing results of specimens of the new and aged specimens at room temperature are given in TABLE 2.

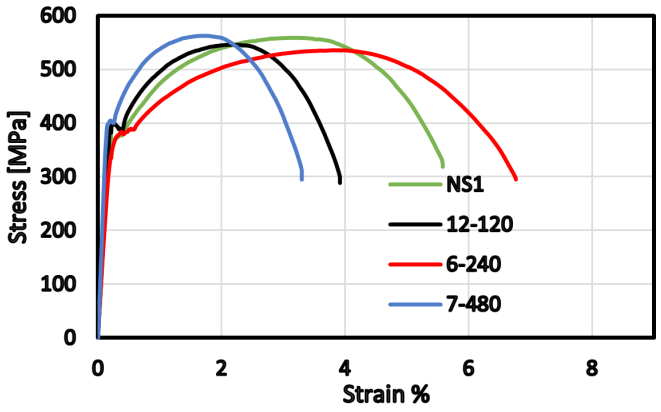

Fig. 3. Stress-strain curves for the tested specimens

TABLE 3

Results of mechanical properties of tensile testing

Ageing period (hours)	Yield strength [MPa]	Tensile strength [MPa]	Young modulus [GPa]
0	373	559	184
120	401	551	200
240	391	539	200
480	404	556	169

According to the results presented in TABLE 4 and Fig. 3 it's easy to note that the yield strength and tensile strength are insensitive to the chosen, short ageing time, as there is no significant change across the different stages of ageing. The yield strength and tensile strength are maintained at all stages of ageing at a value higher than required minimum value of 320 and 460 MPa respectively for the material according to EN 10216–2 Seamless steel tubes for pressure purposes – Technical delivery conditions – Part 2: Non-alloy and alloy steel tubes with specified elevated temperature properties.

3.2. Load- CMOD curves

The load-CMOD curves for the SENT specimens are shown in Fig. 4. No unstable fracture or unstable propagation phenomena, often known as "pop-in" phenomena, were noticed during the loading procedure, and the load remained stable even after reaching its maximum value.

It can be seen from the figure that the maximum loads of the aged specimens are higher than those of the as-received specimens. TABLE 3 present the maximum loads in each specimen. Notably the as-received specimens have higher CMOD at maximum loads compared to creeped specimens. There is no significant difference in the maximum loads among 120, 240 and 480 hours of creep ageing.

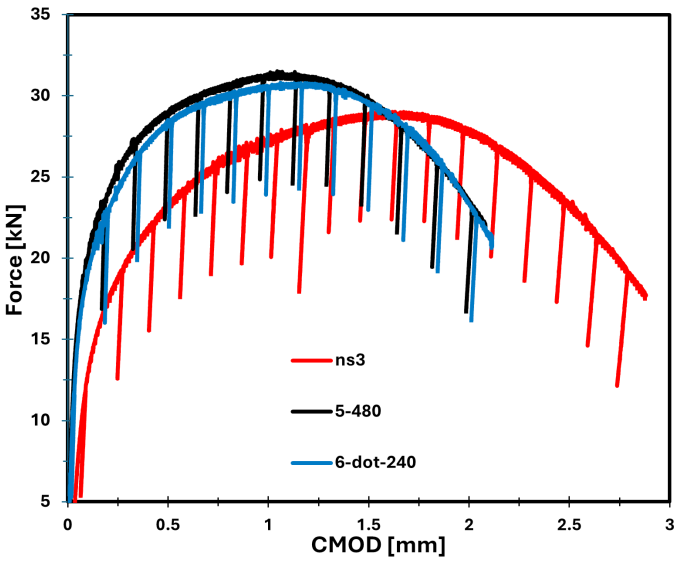

Fig. 4. The records of load vs CMOD curves obtained from the SENT tests of specimens from new, 120, 240 and 480 hours of ageing

3.3. Resistance curves

The UC, DCPD predicted final crack length and the post-mortem measured final crack extension were compared to determine the applicability and reliability of the method of DCPD and UC for crack size assessment as shown in Fig. 5. In some specimens there is a very good correlation between the curves plotted using the UC and the DCPD data.

TABLE 3

Errors in DCPD and UC final crack size measurements

Specimen	N1	N2	N3	10-120	12-120	3-240	6-240	240-6dot	4-480	5-480	7-480
9-point average, mm	1.24	1.757	2.49	1.96	2.14	1.569	1.71	1.77	1.78	1.78	1.75
UC final crack, growth, mm	1.33	2.53	2.82	1.32	1.52	1.50	1.65	1.40	1.46	1.36	1.30
DCPD final crack growth, mm	2.45	2.432	2.3407	2.25	2.4	2.1	1.83	2.21	1.98	2.02	2.19
DCPD % error	97.2	38.43	–6.19	14.77	12.2	33.81	7.44	25.27	10.92	13.5	24.92
UC % error	7.09	44.1	13.04	–32.72	–28.9	–4.12	–3.1	–20.7	–17.99	–23.7	–25.7

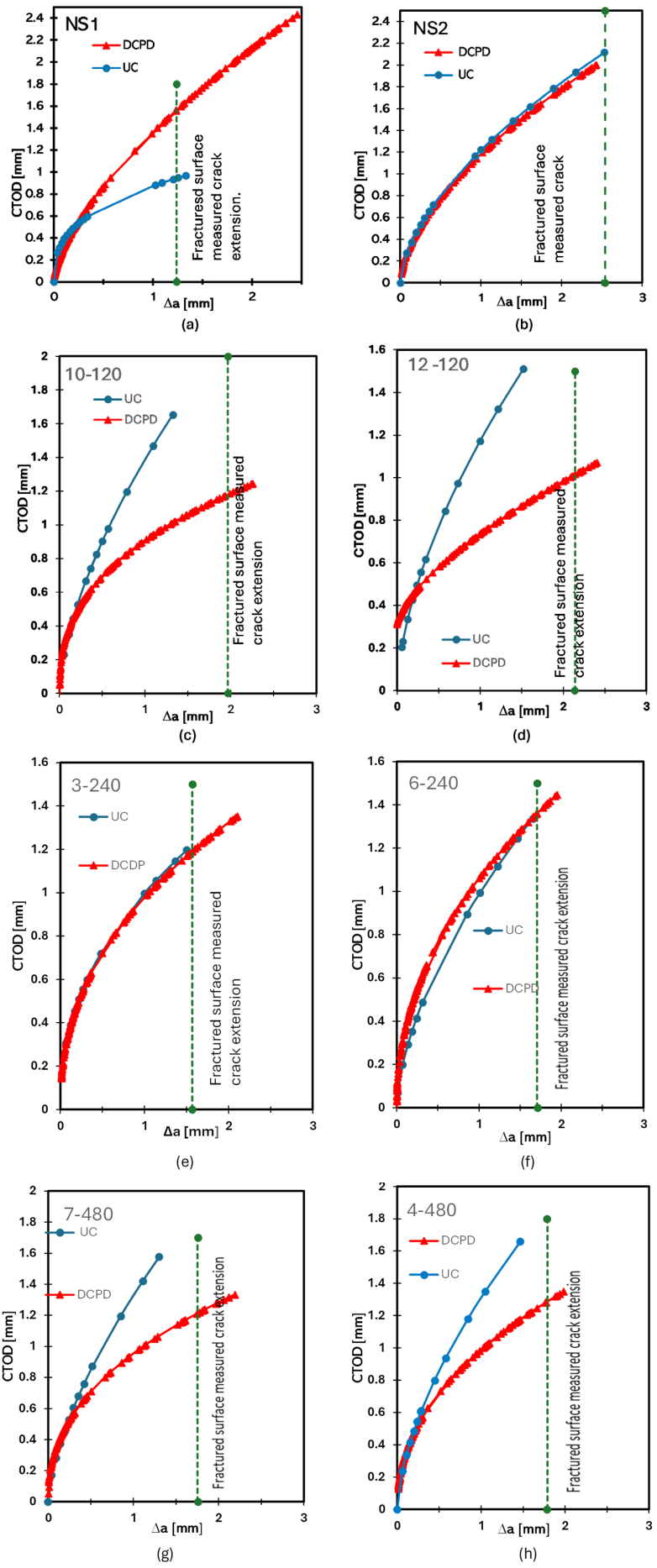

Fig. 5. Resistance curves plotted using UC, and DCPD crack extension

Fig. 6 presents the resistance curves of specimens plotted in one graph plotted using the DCPD data for crack growth. The results showed the trends of superiority of resistance to ductile tearing for new specimens compared to the aged specimens. There is no significant difference in the resistance curves of 120 hours, 240 hours, and 480 hours of ageing. They exhibited similarly lower fracture toughness values.

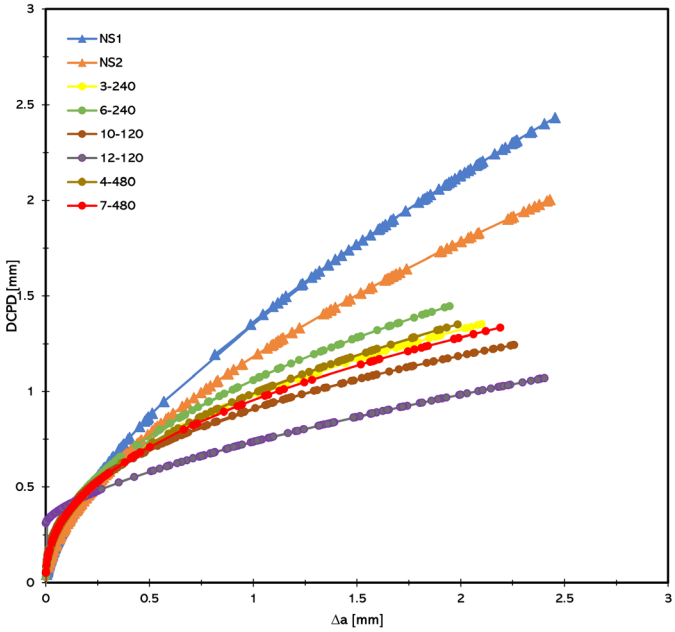

Fig. 6. The resistance curves of specimens plotted in one graph using the DCPD data for crack growth

TABLE 4

Relationship between the ageing stage and maximum loads, crack initiation CTOD and resistance curves efficiencies

Specimen code	Max force (kN)	CTOD-R curve equation, mm
NS1	29.86	$1.3622(\Delta a)^{0.6455}$
NS2	29.02	$1.1815((\Delta a)^{0.5943}$
NS3	29.01	$1.506(\Delta a)^{0.734}$
10-120	31.73	$0.9093(\Delta a)^{0.3856}$
12-120	31.50	$0.3102 + 0.426735(\Delta a)^{0.6592}$
3-240	29.51	$0.977967(\Delta a)^{0.4368}$
6-240	28.66	$1.0602(\Delta a)^{0.4675}$
6DOT-240	30.80	$0.9394(\Delta a)^{0.413154}$
4-480	30.49	$0.9899(\Delta a)^{0.4526}$
5-480	31.51	$0.9222(\Delta a)^{0.400}$
7-480	32.02	$0.954292(\Delta a)^{0.42688}$

TABLE 5

A summary of the average percentage change of measured properties of aged specimens compared to the new as received specimens

	120 hours	240 hours	4 80 hours
% Change of CTOD at Δa0.2 mm	–48%	–39%	–47%
% Change of maximum force	7.9%	1.2%	7%

The equation of the resistance curve shown in TABLE 3 shows the new specimens have coefficient of L greater than 1 in the Equation CTOD = $m + l(\Delta a)^x$. This indicates higher values of CTOD. There is no significant difference in CTOD at crack initiation among the 120, 240 and 480 hours creep aged specimens.

To summarize the results TABLE 5 presents a summary of the average percentage change of measured properties of aged specimens compared to the new as received specimens. Its observable that for all the three stages of ageing the $CTOD_{90}$ parameter was reduced by significant percentage while the maximum load to fracture was the least affected.

According to the findings of the basic mechanical tests reported in TABLE 2 and Fig. 3, yield strength and tensile strength are insensitive to ageing time, since there is no significant change throughout the various phases of ageing. Yield strength and tensile strength are maintained during the ageing process. This is consistent to findings reported in [26]. During the early ageing stage (0-500 h), the precipitation of $M_{23}C_6$ carbide particles strengthens the austenite grain boundaries and twin boundaries while decreasing the solid solution strengthening impact of the austenite grains. The effect of this two phenomena cancel each other, resulting in the aged steel's strength remaining relatively unaltered.

The unloading compliance was found to greatly underestimate the crack size. The crack growth estimations based on unloading compliance most likely might have been affected by the plastic deformation in the specimens' arms. Much of the previous development work for CTOD testing standards was centered on high strength and structural steels, which have relatively high yield strength to ultimate tensile strength (Y/T) ratios ranging from 0.7 to 0.95. For greater strain hardening materials with lower Y/T ratios, such as stainless steel, the conventional CTOD formulae in BS 7448 have been known to be less accurate, that explain the less accuracy of UC in measuring crack length aged specimens. This might be another possible reason because the problem was not experienced in new specimens.

Many tough materials do not fail catastrophically at a specific value of J or CTOD. Instead, these materials exhibit a rising R curve, with J and CTOD increasing with crack growth. Unstable crack propagation is less likely in materials with steep R curves [24].The results indicated that the new specimens have a more rising R-curve as compared to the aged ones. The aged specimens although their R curves are rising less, they still exhibit a degree of stable crack growth and typical resistance curve for a ductile material. This results agree with previous findings in [27] where it was confirmed that the toughness of the material decreases significantly after thermal ageing, which means a lower resistance required during crack propagation.

The difference in values of CTOD values between the new and aged specimens at 0.2 mm crack initiation is because there is a small amount of apparent crack blunting of aged specimens. The new specimens experience a lot of blunting hence higher values of CTOD at crack initiation. The absence of blunting in the aged was explained in [28], where the presence of soft ferrite matrix in the microstructure increase blunting of low alloyed steel at crack tip hence increasing toughness.

The literature [28] reported that the impact toughness of steel which had undergone normalization was made tougher than tempered, quenched and tempered steel while in [29] it was reported that after service period of 168,000 hours at 540°C impact strength remains as satisfactory. Steam line material creep ageing is caused by the progression of precipitation processes, as well as on the growth of grains and the development of microstructure changes and structural discontinuities that result from prolonged exposure to high temperatures. It can therefore be deduced that the near-end life of the operation was not properly imitated. The predominant ductile fracture of 14MoV6-3 steel specimens in the initial condition transforms to predominantly brittle in the aged state. In work [30] an interesting study on Charpy's tests was presented, where force and time were recored. Based on the recorded results authors evaluated energy parameters for crack growth and propagation. Unfortunately, due to the dynamic character of the tests, these parameters cannot be easily linked with the outcome of the presented here approach. A publication [31] reported that impact toughness value of steam line material 14MoV6-3 is primarily determined by the development of precipitation processes, as well as the formation of microstructure alterations and structural discontinuities, as well as grain growth, which occur over a long period of exploitation at extreme temperatures. They reported a very low value of total impact energy (impact toughness) at room temperature 20°C.

In previous studies [32,33] it was reported that microstructure changes characterized by precipitation at grain boundaries occurs after long periods of creep. It was concluded that specimen from new material possesses a coarser surface with large craters with some inclusions and areas of micro voids located inside or around them. Steam line material creep ageing is caused by the progression of precipitation processes, as well as on the growth of grains and the development of microstructure changes and structural discontinuities that result from prolonged exposure to high temperatures.This might be the reason for the observe lack of crack tip blunting prior to crack initiation seen in creeped specimens.

5. Conclusions

The deterioration of CTOD fracture of 14MoV6-3 steel caused by creep was examined by comparing the properties of new and aged steel. Resistance curves of SENT specimens were determined using both the direct current potential drop method and the unloading compliance approach. It was concluded that:

- The specimens show good mechanical properties even after ageing to 480 hours. Yield stress and tensile stress fulfill the standards requirements.
- DCPD provided a better crack prediction compared to UC.
- The character of the curves exclusively changes depending on after ageing but there is no significant difference in CTOD-*R* curves of 120, 240 and 480 hours of ageing.
- The CTOD-*R* curves indicate that new material has high toughness compared to specimens from all the all stages of ageing and their shapes are characteristic of structural metallic materials (rising CTOD-*R* curves). From CTOD-*R* curves, it can be concluded that the crack initiation ranges of new specimens are double that of aged specimens.
- In actual power plants the materials are subjected to multiaxial loading, to this end there is need to investigate the effect of multiaxial loading by use of tilted notches.

Acknowledgments

The study was supported by the Silesian University of Technology within the subsidy for the maintenance and development of research potential 11/030/BK-24/1177 and 11/030/BK-25/1221.

REFERENCES

[1] I. Dzioba, S. Lipiec, I. Dzioba, S. Lipiec, Evolution of the mechanical fields and fracture process of S355JR steel and fracture process Evolution of the mechanical fields of S355JR steel. Procedia Struct. Integr. **16**, 97-104 (2019). DOI: https://doi.org/10.1016/j.prostr.2019.07.027

[2] I. Dzioba, M. Gajewski, A. Neimitz, Studies of fracture processes in Cr e Mo e V ferritic steel with various types of microstructures. Int. J. Press. Vessel. Pip. **87**, 10, 575-586 (2010). DOI: https://doi.org/10.1016/j.ijpvp.2010.07.012.

[3] R. Shaikh, T. Khan, A. Inamdar, M. Jaweed, B. Malik, Review of Fracture Toughness (G, K, J, CTOD, CTOA). IOSR J. Eng. (IOSR JEN) **c**, 62-66, [Online]. Available: http://www.iosrjen.org/.

[4] M. Rund et al., Compatibility of fracture toughness results in the upper shelf region. In Procedia Structural Integrity, The 3rd International Conference on Structural Integrity **17**, 479-486 (2019). DOI: https://doi.org/10.1016/j.prostr.2019.08.063

[5] J.A. Ávila, V. Lima, C.O.F.T. Ruchert, P.R. Mei, A.J. Ramirez, Guide for Recommended Practices to Perform Crack Tip Opening Displacement Tests in High Strength Low Alloy Steels. Soldag. Inspeção **21**, 3, 290-302 (2016).

[6] B. Nyhus, M.L. Polanco, O. Ørjasæther, Sent specimens an alternative to senb specimens. 2019, [Online]. Available: https://www.asme.org/terms-of-use

[7] M. Graba, Numerical analysis of the influence of in-plane constraints on the crack tip opening displacement for sen (b) specimens under predominantly plane strain conditions. Int. J. Appl. Mech. Eng. **21**, 4, 849-866 (2016). DOI: https://doi.org/10.1515/ijame-2016-0050

[8] J. Kowalski, Experimental and numerical investigation on specimen geometry effect on the ctod value for vl-e36 shipbuilding steel. POLISH Marit. Res. **28**, 111, 110-116 (2021).

[9] J. Kang, J.A. Gianetto, W.R. Tyson, Recent development in low-constraint fracture toughness testing for structural integrity assessment of pipelines. Front. Mech. Eng. **13**, 4, 546-553 (2018).

[10] Koen Van Minnebruggen, PhD thesis. Experimental-Numerical Study on the Feasibility of Spirally Welded Pipes in a Strain Based Design Context Koen Van Minnebruggen. Ghent University (2016).

[11] A. Jasiński, A. Zieliński, H. Purzyńska, Pr. Inst. Metal. Żelaza **70**, 3, 2-10 (2018). DOI: https://doi.org/10.32730/imz.0137-9941.18.3.1

[12] D.R.H. Jones, Creep failures of overheated boiler , superheater and reformer tubes. Eng. Fail. Anal. **11**, 873-893 (2004). DOI: https://doi.org/10.1016/j.engfailanal.2004.03.001

[13] M. Jakubowska, A. Wrobel, W. Manaj, A. Sypien, Degradation of microstructure and strength properties of heat-resistant steels operating under variable loads. Int. J. Press. Vessel. Pip. 104916 (2023). DOI: https://doi.org/10.1016/j.ijpvp.2023.104916

[14] I. Čamagić, S.A. Sedmak, A. Sedmak, Z. Burzić, M. Aranđelović, The impact of the temperature and exploitation time on the tensile properties and plain strain fracture toughness, KIc in characteristic areas of welded joint. Frat. ed Integrita Strutt. **12**, 46, 371-382 (2018). DOI: https://doi.org/10.3221/IGF-ESIS.46.34

[15] E.C.F. Standardization, En 13480-2. European Union, p. 1-56 (2002).

[16] G. Sasikala, S.K. Ray, Evaluation of quasistatic fracture toughness of a modified 9Cr-1Mo P91) steel. Mater. Sci. Eng. **479**, A, 105-111 (2008). DOI: https://doi.org/10.1016/j.msea.2007.06.021

[17] M.A. Verstraete, W.De Waele, K. Van Minnebruggen, S. Hertel, International Journal of Pressure Vessels and Piping Crack growth characterization in single-edge notched tension testing by means of direct current potential drop measurement. **156**, 68-78 (2017). DOI: https://doi.org/10.1016/j.ijpvp.2017.06.009

[18] B.S. Publication, BSI Standards Publication Method of test for determination of fracture toughness in metallic materials using single edge notched tension (SENT). BS 8571:2014, 2014

[19] S. Cravero, C. Ruggieri, Estimation procedure of J-resistance curves for SE (T) fracture specimens using unloading compliance. Eng. Fract. Mech. **74**, 2735-2757 (2007). DOI: https://doi.org/10.1016/j.engfracmech.2007.01.012

[20] E. Wang, W. De Waele, S. Hertelé, A complementary ηpl approach in J and CTOD estimations for clamped SENT specimens. Eng. Fract. Mech. **147**, 36-54 (2015). DOI: https://doi.org/10.1016/j.engfracmech.2015.07.043

[21] M.A. Verstraete, W. De Waele, R.M. Denys, K. Van Minnebruggen, S. Hertelé, Constraint analysis of defects in strength mismatched girth welds of (pressurized) pipe and Curved Wide Plate tensile test specimens. Eng. Fract. Mech. **131**, 128-141 (2014). DOI: https://doi.org/10.1016/j.engfracmech.2014.07.018

[22] M.A. Verstraete, S. Hertelé, R.M. Denys, K. Van Minnebruggen, W. De Waele, Evaluation and interpretation of ductile crack extension in SENT specimens using unloading compliance technique. Eng. Fract. Mech. **115**, 190-203 (2014). DOI: https://doi.org/10.1016/j.engfracmech.2013.11.004

[23] G. Shen, J.A. Gianetto, W.R. Tyson, Measurement of J-R Curves Using Single-Specimen Technique on Clamped SE (T) Specimens. In Proceedings of the Nineteenth (2009) International Offshore and Polar Engineering Conference **1**, 880653 (2009).

[24] Ted. L. Anderson, Fracture mechanics Fundamentals and Applications, Third Edit. Taylor & Francis Group, (2005).

[25] ASTM E8/E8M − 13a, Standard Test Methods for Tension Testing of Metallic Materials 1. USA, (2013).

[26] G. Chen, J. Liu, J. Wang, T. Zhang, Effect of high temperature aging on microstructure and mechanical properties of HR3C heat resistant steel. Energy Mater. Mater. Sci. Eng. Energy Syst. **9**, 2, 205-210 (2014). DOI: https://doi.org/10.1179/1743284713Y.0000000347

[27] S. Wu, Z. Zhang, Long term ageing effect on fracture toughness of the GTAW welded joints for nuclear power main pipelines. Int. J. Press. Vessel. Pip. 188, November, 104250 (2020). DOI: https://doi.org/10.1016/j.ijpvp.2020.104250.

[28] E.S. Ameh, B.O. Onyekpe, Effect of High Strength Steel Microstructure on Crack Tip Opening Displacement. Am. J. Eng. Res. **78**, 7, 72-78 (2016).

[29] J. Ćwiek, J. Łabanowski, S. Topolska, The effect of long-term service at elevated temperatures on structure and mechanical properties of Cr-Mo-V steel. Arch. Mater. Sci. Eng. 49, 1, 33-39, (2011).

[30] B.Z.E. Čević, A. Maksimović, L. Milović, S. Bulatović, V. Aleksić, Effect of temperature and specimen orientation on Charpy impact toughness toughness. Procedia Struct. Integr. **42**, 1475-1482 (2022). DOI: https://doi.org/10.1016/j.prostr.2022.12.188

[31] D. Hodži, I. Hajro, Impact toughness of steamline material 14MoV6-3 after long-term exploitation. In 14th International Research/Expert Conference. "Trends in the Development of Machinery and Associated Technology," **3**, September, 129-132 (2010).

[32] A. Zieliński, Assessment of loss in life time of the primary steam pipeline material after long-term service under creep conditions. J. Achiev. Mater. Manuf. Eng. **54**, 1, 67-74 (2012).

[33] I.C. Alagic, Microstructural morphology effects on fracture resistance and crack tip strain distribution in Ti–6Al–4V alloy for orthopedic implant. Mater. Des. **53**, 870-880 (2014).